Bottom Ekman Pumping with Stress-Dependent Eddy Viscosity

BENOIT CUSHMAN-ROISIN

Thayer School of Engineering, Dartmouth College, Hanover, New Hampshire

VLADO MALAČIČ

Marine Biological Station Piran, Piran, Slovenia

(Manuscript received 29 August 1996, in final form 4 March 1997)

ABSTRACT

This paper reconsiders the classic problem of bottom Ekman pumping below a steady geostrophic flow by relaxing the assumption of a constant eddy viscosity. It is assumed instead that the eddy viscosity depends on the magnitude of the bottom stress, which itself is a function of the geostrophic flow. Results show that the vertical Ekman pumping is no longer directly proportional to the relative vorticity of the geostrophic flow, but is a far more complicated function of the geostrophic flow. Specific examples are discussed, which show that the Ekman pumping rate may be 50% or 100% larger than that predicted by the traditional theory.

1. Introduction

It has long been established that the role of vertical friction in the deep ocean is relegated to relatively thin layers, called Ekman layers. One of these is the bottom Ekman layer, which exists to bring the horizontal velocity components from their finite values in the lower water column to zero at the bottom. The combination of Coriolis and frictional forces in the Ekman layer creates a substantial veering, and there exists in the layer a flow component transverse to the current aloft. Thus, although that current may be in geostrophic balance and almost nondivergent, the transverse flow in the Ekman layer is divergent or convergent. Continuity of fluid demands a compensating vertical velocity, which extends through the water column. This is called Ekman pumping.

Ekman pumping is important for several reasons. First, it plays a significant dynamical role by stretching or squeezing the ocean's interior flow; this, in turn, affects the vorticity of the ocean circulation. Second, slow but persistent vertical velocities are essential in transporting chemicals, contaminants (such as radioactive wastes), and nutrients through the water column, and in controlling their residency time.

According to the traditional theory, which relies on the assumption of a uniform eddy viscosity (see, e.g., Pedlosky 1987, chapter 4; Cushman-Roisin 1994, chapter 5), there is a direct proportionality between the transverse velocity component in the Ekman layer and the overlying geostrophic velocity, and it is found that the Ekman pumping rate is proportional to the relative vorticity of the geostrophic flow. Thus, for example, a cyclonic gyre in the ocean's interior is associated with convergent flow in the bottom Ekman layer and an upward vertical velocity proportional to the gyre's local relative vorticity. It is well known, however, that the turbulent state of the ocean's bottom boundary layer is such that the eddy viscosity is not vertically uniform but varies significantly with distance above the bottom (Weatherly and Martin 1978). The magnitude of the eddy viscosity also varies horizontally with the local bottom stress. While the vertical profile of the eddy viscosity controls the structure of the current distribution through the Ekman layer, its magnitude controls characteristics such as the thickness of the layer. The magnitude of the transverse transport depends on the overlying geostrophic flow speed and on the thickness of the layer, which varies with the eddy viscosity, the bottom stress, and thus the geostrophic flow speed itself. In sum, the transverse transport is more than proportional to the overlying geostrophic current, and the Ekman-pumping velocity cannot be simply proportional to the vorticity of the geostrophic flow but must depend on it in some more complicated, nonlinear way. Our objective here is to determine this relationship between Ekman pumping and geostrophic flow when a more realistic eddy viscosity parameterization than a constant is adopted.

Corresponding author address: Dr. Benoit Cushman-Roisin, Thayer School of Engineering, Dartmouth College, 8000 Cummings Hall, Hanover, NH 03755-8000.
E-mail: B.Cushman@dartmouth.edu

© 1997 American Meteorological Society

A classic parameterization of the eddy viscosity in a sheared boundary layer[1] is (Ellison 1956)

$$\nu = \kappa u_* z, \tag{1}$$

where ν is the eddy viscosity, $\kappa = 0.40$ the von Kármán constant of turbulence, u_* the so-called friction velocity, and z the distance from the boundary. The friction velocity is defined from the boundary stress τ_b according to

$$\tau_b = \rho u_*^2, \tag{2}$$

where ρ is the fluid's density. The virtues of this relatively simple parameterization are its increase with distance from the boundary and its increase with the amount of shear stress, according to results of laboratory experiments and geophysical observations. It has been used in numerous studies of homogeneous rotating flows: among others, Ellison (1956) in a study of turbulence in the atmospheric boundary layer, Madsen (1977) in a study of the ocean's wind-driven surface Ekman layer, and Nihoul (1977), Lavelle and Mofjeld (1983), Ostendorf (1984), and Soulsby (1990) in studies of tidal currents in shallow well-mixed waters. The solution is in terms of Kelvin–Thomson functions (a variety of Bessel functions because of the proportionality of ν to z) and is well known. In all these studies, however, the dependency of the eddy viscosity on the friction velocity is treated parameterically, and no one to our knowledge has yet investigated its effect on Ekman pumping in the deep ocean. To fill this gap, we investigate here how parameterization (1)–(2) for the eddy viscosity modifies the expression for the Ekman pumping generated by bottom friction in the deep ocean.

The study of Weatherly and Martin (1978), based on a turbulence-closure model, reveals that the eddy viscosity in the ocean's benthic layer behaves according to (1) near the bottom but reaches a maximum at some height and decreases nearly exponentially with farther distance from the bottom. An improved parameterization with exponential attenuation has been proposed (Long 1981), but the intractability of the ensuing mathematical problem demands numerical solution. Adopting such refined parameterization in our study would preclude the derivation of an analytical formula for the Ekman pumping rate, and we decided not to go beyond (1)–(2). It is also expected that the difference would be minor since values of the eddy viscosity significantly away from the bottom where the velocity shear is small are nearly irrelevant, and the structure of the boundary layer is essentially governed by the behavior of the eddy viscosity near the bottom where the velocity shear is greatest. This assertion is verified a posteriori.

Our work is structured in the following way. Section 2 briefly reviews the solution of the Ekman-layer equations with eddy viscosity parameterized by (1)–(2) and recapitulates its advantages over that with constant eddy viscosity. Section 3 then derives from this solution a new formula giving the vertical Ekman-pumping velocity in the ocean's interior in terms of its geostrophic velocity. Several particular cases are considered and discussed. The concluding section 4 highlights the differences with the predictions of the traditional theory based on constant eddy viscosity. At the end of the paper is a short appendix defining two particular functions derived from the Kelvin–Thomson functions that facilitate the analytical developments.

2. Bottom Ekman layer

a. Equations and boundary conditions

Traditional Ekman dynamics include a balance between the Coriolis, pressure gradient, and vertical-friction forces. Time derivatives and nonlinear advective terms can also be incorporated (Soulsby 1990; Hart 1995), but we shall not to do so in order to restrict the attention to the effect of a varying eddy viscosity on Ekman pumping. Also, our new parameterization of Ekman pumping would be most useful in general circulation studies, when geostrophy is an excellent approximation.

Above the Ekman layer, the frictional force vanishes and the balance of forces reduces to geostrophy; by virtue of the homogeneity of the fluid and of the hydrostatic balance, which we also assume, the horizontal pressure gradient is depth independent, and we write

$$-f(v - \bar{v}) = \frac{\partial}{\partial z}\left(\kappa u_* z \frac{\partial u}{\partial z}\right) \tag{3a}$$

$$+f(u - \bar{u}) = \frac{\partial}{\partial z}\left(\kappa u_* z \frac{\partial v}{\partial z}\right), \tag{3b}$$

where f is the Coriolis parameter (assumed constant and positive), u and v the horizontal velocity components within the layer ($0 \leq z$), $\bar{u}$ and $\bar{v}$ the geostrophic flow aloft ($z \to \infty$), and $\kappa u_* z$ the variable eddy viscosity presented earlier. We employ partial derivatives with respect to the vertical coordinate z because we consider the geostrophic flow $(\bar{u}, \bar{v})$ to be varying horizontally (in x and y directions) and to induce horizontal variability in u, v, and u_*. Boundary conditions are

Top of Ekman layer:

$$u \to \bar{u}, \qquad v \to \bar{v}, \quad \text{as } z \to \infty \tag{4}$$

Bottom of Ekman layer:

$$u = 0, \qquad v = 0, \quad \text{at } z = z_0. \tag{5}$$

In the bottom boundary conditions, it is necessary to distinguish the level $z = z_0$, where z_0 is the roughness height, from the average bottom level $z = 0$, because of the singularity of the anticipated logarithmic velocity profile in the near-bottom zone (e.g., Lavelle and Mofjeld 1983).

[1] The turbulent Ekman layer is none other than a sheared boundary layer in the presence of rotation.

Governing equations (3a,b) form a fourth-order problem, which together with the four boundary conditions in (4)–(5) can be solved uniquely. In that solution, however, the friction velocity u_* will appear parameterically, and it will be necessary to close the problem by relating this parameter to the magnitude of the bottom stress via (2); that is,

$$\rho u_*^2 = \tau_b = \sqrt{\tau_x^2 + \tau_y^2}, \tag{6}$$

where τ_x and τ_y are the bottom stress components. Since these implicate the velocity components as well as the friction velocity, it is at this stage that a nonlinearity will be introduced in the mathematical formalism.

b. Solution

Using the functions $a(\zeta)$ and $b(\zeta)$ derived in the appendix from the decaying Kelvin–Thomson functions, the solution of (3a,b) that meets the upper boundary conditions (4) is

$$u = \bar{u} + Aa\left(\frac{fz}{\kappa u_*}\right) + Bb\left(\frac{fz}{\kappa u_*}\right) \tag{7a}$$

$$v = \bar{v} - Ba\left(\frac{fz}{\kappa u_*}\right) + Ab\left(\frac{fz}{\kappa u_*}\right), \tag{7b}$$

where A and B are two constants of integration. These constants are to be determined by applying the remaining two boundary conditions, namely (5). Since the level $z = z_0$ is very close to the average bottom level $z = 0$ (usually less than a millimeter; Soulsby 1990), it can be assumed that the dimensionless quantity $fz_0/\kappa u_*$ is much smaller than unity, and the asymptotic behaviors of a and b near the origin can be used [see (A6a) and (A7a)]. It follows that

$$0 = \bar{u} + A\left[-\frac{1}{2}\ln\frac{fz_0}{\kappa u_*} - \gamma\right] - \frac{\pi}{4}B \tag{8a}$$

$$0 = \bar{v} - B\left[-\frac{1}{2}\ln\frac{fz_0}{\kappa u_*} - \gamma\right] - \frac{\pi}{4}A, \tag{8b}$$

where $\gamma = 0.57722$ is the Euler constant. The solution is immediate;

$$A = \frac{4}{\pi(1+\lambda^2)}(\bar{v} - \lambda\bar{u}) \tag{9a}$$

$$B = \frac{4}{\pi(1+\lambda^2)}(\bar{u} + \lambda\bar{v}), \tag{9b}$$

where the coefficient λ, defined by

$$\lambda = \frac{4}{\pi}\left(\frac{1}{2}\ln\frac{\kappa u_*}{fz_0} - \gamma\right), \tag{10}$$

has been introduced for convenience. Note that, because the logarithm is a weak function of its argument, the coefficient λ is a weak function of the friction velocity u_*.

With u_* remaining as a parameter, the solution is

$$u = \bar{u} + \frac{4}{\pi(1+\lambda^2)}(\bar{v} - \lambda\bar{u})a\left(\frac{fz}{\kappa u_*}\right) + \frac{4}{\pi(1+\lambda^2)}(\bar{u} + \lambda\bar{v})b\left(\frac{fz}{\kappa u_*}\right) \tag{11a}$$

$$v = \bar{v} - \frac{4}{\pi(1+\lambda^2)}(\bar{u} + \lambda\bar{v})a\left(\frac{fz}{\kappa u_*}\right) + \frac{4}{\pi(1+\lambda^2)}(\bar{v} - \lambda\bar{u})b\left(\frac{fz}{\kappa u_*}\right). \tag{11b}$$

Collecting separately the terms proportional to $\bar{u}$ and $\bar{v}$, we can write the same solution in the form

$$u = \left[1 + \frac{4(b - \lambda a)}{\pi(1+\lambda^2)}\right]\bar{u} + \frac{4(a + \lambda b)}{\pi(1+\lambda^2)}\bar{v} \tag{12a}$$

$$v = \left[1 + \frac{4(b - \lambda a)}{\pi(1+\lambda^2)}\right]\bar{v} - \frac{4(a + \lambda b)}{\pi(1+\lambda^2)}\bar{u}, \tag{12b}$$

which reveals the components of the flow that are parallel and transverse to the geostrophic current. We note that the transverse component, equal in magnitude to the absolute value of $4(a + \lambda b)/\pi(1 + \lambda^2)$ times the speed of the geostrophic current, is not proportional to the latter; indeed, the parameter λ includes a dependency on the friction velocity, which will shortly be related to the geostrophic current speed.

c. Friction velocity

We now close the problem and determine the friction velocity u_* by relating it to the actual bottom stress. First, the bottom-stress components are calculated:

$$\tau_x = \lim_{z\to 0}\left(-\rho\kappa u_* z\frac{\partial u}{\partial z}\right) = -\frac{4\rho\kappa u_*}{\pi(1+\lambda^2)}\left[(\bar{v} - \lambda\bar{u})\lim_{\zeta\to 0}\left(\zeta\frac{da}{d\zeta}\right) + (\bar{u} + \lambda\bar{v})\lim_{\zeta\to 0}\left(\zeta\frac{db}{d\zeta}\right)\right] \tag{13a}$$

$$\tau_y = \lim_{z\to 0}\left(-\rho\kappa u_* z\frac{\partial v}{\partial z}\right) = +\frac{4\rho\kappa u_*}{\pi(1+\lambda^2)}\left[(\bar{u} + \lambda\bar{v})\lim_{\zeta\to 0}\left(\zeta\frac{da}{d\zeta}\right) - (\bar{v} - \lambda\bar{u})\lim_{\zeta\to 0}\left(\zeta\frac{db}{d\zeta}\right)\right], \tag{13b}$$

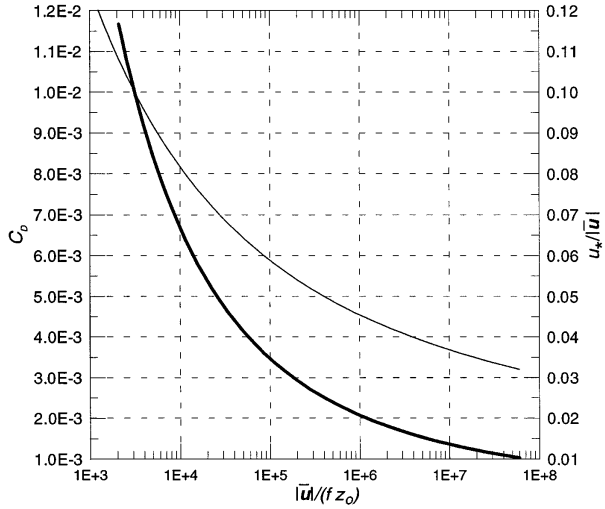

FIG. 1. Variation of the friction velocity u_* (thin line) and drag coefficient C_D (thick line) with the geostrophic current speed $|\bar{\mathbf{u}}|$.

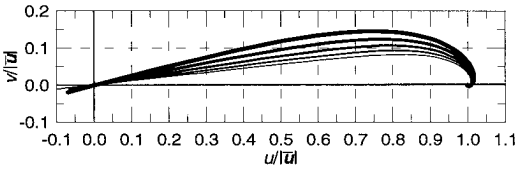

FIG. 2. Ekman spirals for various values of the dimensionless ratio $|\bar{u}|/fz_0$, where $|\bar{u}|$ is the speed of the geostrophic current above the Ekman layer, f the Coriolis parameter, and z_0 is the roughness height. The uppermost and thickest line corresponds to $|\bar{u}|/fz_0 = 10^4$, and every successively thinner line to a value 10 times larger, with the lowest and thinnest line corresponding to $|\bar{u}|/fz_0 = 10^8$. The point where the spirals curl represents the geostrophic flow aloft, while the origin is crossed at level z_0. The branches in the third quadrant, beyond the origin, exist because of the logarithmic nature of the velocity profiles but are physically meaningless.

where ζ is $fz/\kappa u_*$. The limits (A7b,c) established in the appendix yield

$$\tau_x = +\frac{2\rho\kappa u_*}{\pi(1+\lambda^2)}(\bar{v} - \lambda\bar{u}) \tag{14a}$$

$$\tau_y = -\frac{2\rho\kappa u_*}{\pi(1+\lambda^2)}(\bar{u} + \lambda\bar{v}). \tag{14b}$$

The friction velocity u_* can then be derived from (6) as

$$\rho u_*^2 = \frac{2\rho\kappa u_*}{\pi(1+\lambda^2)}\sqrt{(\bar{v} - \lambda\bar{u})^2 + (\bar{u} + \lambda\bar{v})^2},$$

which can be reduced to

$$u_* = \frac{2\kappa}{\pi}\sqrt{\frac{\bar{u}^2 + \bar{v}^2}{1+\lambda^2}} = \frac{2\kappa|\bar{\mathbf{u}}|}{\pi\sqrt{1+\lambda^2}}. \tag{15}$$

Since the parameter λ, defined in (10), includes u_*, formula (15) is an implicit[2] equation for the friction velocity, in terms of the magnitude of the geostrophic flow $|\bar{\mathbf{u}}| = \sqrt{\bar{u}^2 + \bar{v}^2}$, the roughness height z_0, the Coriolis parameter f, and dimensionless constants. The thin curve in Fig. 1 traces the value of $u_*/|\bar{\mathbf{u}}|$ versus $|\bar{\mathbf{u}}|/fz_0$. Credit for relationship (15) between the friction velocity and the geostrophic speed goes to Ellison [1956, his Eq. (15) and his Table 2].

d. Bottom stress and drag coefficient

Expressions (14a,b) show that the bottom stress consists of a component antiparallel to the geostrophic current (acting as a retarding force) and a transverse component. The ratio of these components is λ^{-1}, which yields the angle of deflection between the geostrophic current and its associated bottom stress.

From the magnitude of the bottom stress, we can derive a drag coefficient by writing

$$\tau_b = \sqrt{\tau_x^2 + \tau_y^2} = C_D\rho|\bar{\mathbf{u}}|^2, \tag{16}$$

with

$$C_D = \frac{4\kappa^2}{\pi^2(1+\lambda^2)}. \tag{17}$$

Since λ contains a weak dependency upon u_* according to (10), with u_* itself depending upon the speed of the geostrophic flow $|\bar{\mathbf{u}}|$ according to (15), this drag coefficient is not constant but a function of the dimensionless, Rossby-like number $|\bar{\mathbf{u}}|/fz_0$. [In the atmospheric boundary layer literature, this number is occasionally called the surface Rossby number (e.g., Garratt 1992, p. 44)]. The variation is shown by the thick line in Fig. 1. Expression (17) is not new but was first derived by Ellison (1956) and again by Lavelle and Mofjeld (1983). These last authors also compared its predictions with a variety of estimated values derived from measurements taken in the ocean's benthic boundary layer and found good agreement (see their Fig. 9). This agreement spurs us on to derive later an expression for the Ekman pumping under the present choice of eddy-viscosity parameterization.

e. Veering angle and thickness of Ekman layer

Figure 2 shows velocity hodographs according to solution (11a,b), in which the parameter λ and the friction velocity u_* are related to the geostrophic speed $|\bar{\mathbf{u}}|$, the roughness height z_0, and the Coriolis parameter f by (10) and (15). Since this solution contains the free dimensionless number $|\bar{\mathbf{u}}|/fz_0$, there is a family of hodographs, all Ekman spirals but of various widths. Regardless of the value of $|\bar{\mathbf{u}}|/fz_0$, the transverse flow (to the left in the Northern Hemisphere, to the right in the Southern Hemisphere) hardly exceeds 10% of the geostrophic

[2] This implicit relation can, however, be inverted, and $|\bar{\mathbf{u}}|/fz_0$ can be expressed as an explicit function of $u_*/|\bar{\mathbf{u}}|$. In the process, a square root must be taken; physics dictate that the root corresponding to the lower velocity values be selected.

flow, unlike in the traditional solution according to which it reaches 32%.[3]

If the veering angle α is defined as the angle between the current as z approaches zero and the geostrophic current aloft, Eqs. (12a–b) yield

$$\tan\alpha = \lim_{z\to 0} \frac{-4(a + \lambda b)}{\pi(1 + \lambda^2) + 4(b - \lambda a)} = \frac{1}{\lambda}. \quad (18)$$

Table 1 lists selected values for a wide range of Rossby-like numbers. As we can readily note, all values are significantly lower than the traditional value of 45°. In numerical simulations of the oceanic bottom boundary layer with a turbulence-closure model, Ezer and Weatherly (1990) found α values of $10° \pm 2°$ with $f = 9.47 \times 10^{-5}$ s^{-1} (latitude 40.5° N), $z_0 = 1.6 \times 10^{-4}$ m, and a geostrophic velocity above the Ekman layer of 10 cm s^{-1}. For the same parameter values, the present model yields an angle of 8.6°.

A question that arises naturally is: How thick is the Ekman layer? Taking the top of the layer as the level above which the vector velocity does not differ from the geostrophic current by more than 5%, we write

$$\sqrt{\frac{(u - \bar{u})^2 + (v - \bar{v})^2}{\bar{u}^2 + \bar{v}^2}} = \varepsilon$$

at $z = d$, where $\varepsilon = 0.05$ and d is the nominal layer thickness. Use of solution (11a,b) yields an implicit equation for d:

$$a^2\left(\frac{fd}{\kappa u_*}\right) + b^2\left(\frac{fd}{\kappa u_*}\right) = \frac{\pi^2(1 + \lambda^2)}{16}\varepsilon^2. \quad (19)$$

Table 1 lists solutions for five different values of the Rossby-like number $|\bar{\mathbf{u}}|/fz_0$.

Before closing this section, we return to our choice of parameterization of eddy viscosity and show that the ever-increasing value of ν with z (while a more realistic parameterization would have a saturating or even decaying value far above the bottom) has no perceptible impact on the solution. There are several ways to prove this assertion. The first one is to remark that all properties derived from the present solution (friction velocity, drag coefficient, veering angle, layer thickness, and, later, Ekman pumping) depend solely on the properties (A7a,b,c) and (A8a,b) of the building-block functions $a(\zeta)$ and $b(\zeta)$. While the behavior near the origin (A7a,b,c) is directly controlled by the logarithmic singularity, which would remain unchanged as long as $\nu(z)$ behaves like z near the origin, the integral properties (A8a,b) too do not depend on the detailed structure of z but only on the requirement that the functions vanish at infinity and again on the behavior near the origin. Therefore, values of ν away from the origin are inconsequential.

Another way of arriving at the same conclusion is to consider numerical values. Since the decay of velocity deficit (velocity minus geostrophic flow) at the top of the boundary layer is exponential, the 5% departure criterion truly captures most of the extent of the boundary layer. The values listed in Table 1 can then be used to estimate the "final" values of $\nu(z)$ that matter, and with $d = (0.235\text{–}0.663)u_*/f$, we find successively $\nu_{\text{top}} = \kappa u_* d = (0.094\text{–}0.265)u_*^2/f = (9.12\ 10^{-5}\text{–}1.77\ 10^{-3})|\bar{\mathbf{u}}|^2/f$. With a large $|\bar{\mathbf{u}}|$ value of about 10 cm s^{-1} and $f = 10^{-4}$ s^{-1}, the range is 91.2–1770 cm^2 s^{-1}, all in the realm of inferred values for the ocean bottom. [For example, in the Celtic Sea with $u_* \approx 2$ cm s^{-1}, Soulsby (1990) estimated eddy viscosity values as large as 1100 cm^2 s^{-1} where the parameterization $\nu(z) = \kappa u_* z$ still holds.]

3. Ekman pumping

The volumetric transport carried by the velocity deficit in the boundary layer has components given by

$$U = \int_0^\infty (u - \bar{u})\, dz = \frac{4\kappa u_*}{\pi(1 + \lambda^2)f}\left[(\bar{v} - \lambda\bar{u})\int_0^\infty a(\zeta)\, d\zeta + (\bar{u} + \lambda\bar{v})\int_0^\infty b(\zeta)\, d\zeta\right] \quad (20a)$$

$$V = \int_0^\infty (v - \bar{v})\, dz = \frac{4\kappa u_*}{\pi(1 + \lambda^2)f}\left[(\bar{v} - \lambda\bar{u})\int_0^\infty b(\zeta)\, d\zeta - (\bar{u} + \lambda\bar{v})\int_0^\infty a(\zeta)\, d\zeta\right]. \quad (20b)$$

Integral relations (A8a,b) yield

$$U = -\frac{2\kappa u_*(\bar{u} + \lambda\bar{v})}{\pi(1 + \lambda^2)f}, \qquad V = -\frac{2\kappa u_*(\bar{v} - \lambda\bar{u})}{\pi(1 + \lambda^2)f}. \quad (21a,b)$$

This Ekman layer transport is perpendicular to the bottom stress vector given by (14a,b) and is at an angle $\pi - \tan^{-1}\lambda$ to the left of the geostrophic current (in the Northern Hemisphere, since we chose f to be positive). More importantly, it is not a linear but a nearly quadratic function of the geostrophic current.

The Ekman-pumping vertical velocity in the geo-

[3] This percentage is the maximum value of $e^{-z}\sin z$, the ratio of the transverse velocity to the geostrophic speed in the traditional Ekman-layer theory (obtained for $z = \pi/4$).

TABLE 1. Veering angle and thickness of the Ekman layer for various values of the geostrophic current speed and roughness height.

Surface Rossby number $\frac{\lvert\bar{\mathbf{u}}\rvert}{fz_0}$	Veering angle α	Ekman-layer thickness d
10^4	18.7°	$0.663\frac{u_*}{f} = 5.42\ 10^{-2}\frac{\lvert\bar{\mathbf{u}}\rvert}{f} = 5.42\ 10^2 z_0$
10^5	13.4°	$0.489\frac{u_*}{f} = 2.88\ 10^{-2}\frac{\lvert\bar{\mathbf{u}}\rvert}{f} = 2.88\ 10^3 z_0$
10^6	10.3°	$0.374\frac{u_*}{f} = 1.70\ 10^{-2}\frac{\lvert\bar{\mathbf{u}}\rvert}{f} = 1.70\ 10^4 z_0$
10^7	8.31°	$0.294\frac{u_*}{f} = 1.09\ 10^{-2}\frac{\lvert\bar{\mathbf{u}}\rvert}{f} = 1.09\ 10^5 z_0$
10^8	6.95°	$0.235\frac{u_*}{f} = 7.32\ 10^{-3}\frac{\lvert\bar{\mathbf{u}}\rvert}{f} = 7.32\ 10^5 z_0$

strophic interior is obtained from a vertical integration of the three-dimensional continuity equation:

$$\bar{w} = -\left(\frac{\partial U}{\partial x} + \frac{\partial V}{\partial y}\right) = \frac{2\kappa}{\pi f}\left[\frac{\partial}{\partial x}\left(\frac{u_*(\bar{u} + \lambda\bar{v})}{1 + \lambda^2}\right) + \frac{\partial}{\partial y}\left(\frac{u_*(\bar{v} - \lambda\bar{u})}{1 + \lambda^2}\right)\right], \quad (22)$$

where the intermediate variables u_* and λ are nonlinearly related to the geostrophic flow $(\bar{u}, \bar{v})$ via Eqs. (10) and (15). Formula (22) for the Ekman-pumping rate is the main result of this paper. It differs from the traditional expression for the Ekman pumping (e.g., Pedlosky 1987, sections 4–5; Cushman-Roisin 1994, sections 5–3):

$$\bar{w} = \sqrt{\frac{\nu}{2f}}\left(\frac{\partial\bar{v}}{\partial x} - \frac{\partial\bar{u}}{\partial y}\right), \quad (23)$$

where ν is the eddy viscosity, then assumed to be a constant.

Because the logarithmic function in (10) prevents us from solving (10)–(15) explicitly for u_* and λ, it is difficult to quantify precisely the difference between the predictions of (22) and (23). However, because the logarithm is a weak function of its argument, the parameter λ given by (10) may be approximated to a constant. With this approximation the friction velocity u_* becomes simply proportional to the geostrophic speed $|\bar{\mathbf{u}}|$, according to (15). (Note that the variation of the ratio $u_*/|\bar{\mathbf{u}}|$ shown in Fig. 1 is displayed on a logarithmic–linear scale; thus, for a fixed value of the roughness height z_0, variations of the geostrophic speed within an order of magnitude imply minor variations of the ratio $u_*/|\bar{\mathbf{u}}|$.) The corresponding expression for the Ekman-pumping rate is

$$\bar{w} = \frac{4\kappa^2}{\pi^2(1 + \lambda^2)^{3/2} f}\left[\frac{\partial}{\partial x}\left[|\bar{\mathbf{u}}|(\bar{u} + \lambda\bar{v})\right] + \frac{\partial}{\partial y}\left[|\bar{\mathbf{u}}|(\bar{v} - \lambda\bar{u})\right]\right]. \quad (24)$$

Then, taking the derivatives of the individual factors and recalling that a geostrophic flow is nondivergent on the f plane (i.e., $\partial\bar{u}/\partial x + \partial\bar{v}/\partial y = 0$), we obtain

$$\bar{w} = \frac{4\kappa^2\lambda|\bar{\mathbf{u}}|}{\pi^2(1 + \lambda^2)^{3/2} f}\left(\frac{\partial\bar{v}}{\partial x} - \frac{\partial\bar{u}}{\partial y}\right) + \frac{4\kappa^2}{\pi^2(1 + \lambda^2)^{3/2} f|\bar{\mathbf{u}}|}\left[(\bar{u} + \lambda\bar{v})\left(\bar{u}\frac{\partial\bar{u}}{\partial x} + \bar{v}\frac{\partial\bar{v}}{\partial x}\right) + (\bar{v} - \lambda\bar{u})\left(\bar{u}\frac{\partial\bar{u}}{\partial y} + \bar{v}\frac{\partial\bar{v}}{\partial y}\right)\right]. \quad (25)$$

The first term of (25), that on the upper line, is proportional to the vorticity of the geostrophic flow and can be readily identified with the single term of the traditional expression (23). Identification of the respective coefficients yields the resulting bulk eddy viscosity:

$$\nu_{\text{bulk}} = \frac{8\kappa^2\lambda^2}{\pi^2(1 + \lambda^2)^2}\frac{u_*^2}{f}, \quad (26)$$

which can be interpreted as the product of the von Kármán constant κ, the friction velocity u_*, and an effective height proportional to u_*/f. This comes as no surprise since the ratio u_*/f is known to provide the depth scale of the turbulent Ekman layer (Csanady and Shaw 1980) and that scaling was already apparent in the dimensionless argument of the functions a and b in (11a, b) above.

Of much greater interest is the second term of (25), that on the lower line. This term has the same order of magnitude as the first one and is by no account negligible. Yet, it has no counterpart in the classic theory.

In order to highlight some of the differences, we explore four particular cases, namely, those of a unidirectional sheared current, a solid-body rotation, a zero-vorticity circular flow, and a more complex vortex flow.

For a unidirectional shear flow $\bar{u} = 0$, $\bar{v} = \bar{v}(x)$, we readily obtain

$$\bar{w} = \frac{4\kappa^2\lambda|\vec{v}|}{\pi^2(1 + \lambda^2)^{3/2} f}\left(\frac{d\bar{v}}{dx} + \frac{d\bar{v}}{dx}\right), \tag{27}$$

where the first and second terms correspond respectively to the first and second terms of (25). Therefore, in the case of a unidirectional shear flow, the new expression for the Ekman-pumping rate predicts a value twice as large as that predicted by the traditional theory. Physically, the faster the geostrophic flow, the greater the transverse velocity and also the greater the bottom stress, the more energetic the turbulence, and the thicker the Ekman layer (thickness proportional to the local geostrophic velocity, and not constant as the traditional theory would have it). Thus, the transverse volumetric transport is not linearly but quadratically depending on the geostrophic current. This quadraticity accounts for the factor 2.

In their numerical simulations of an oceanic bottom boundary layer, Ezer and Weatherly (1990) discussed Ekman pumping under a lateral velocity gradient of 3.3 cm s^{-1} over a distance of 10 km (i.e., $d\bar{v}/dx = 3.3 \times 10^{-6}$ s^{-1}) when the turbulent eddy viscosity reached values of about 70 cm^2 s^{-1} (at 40.5° N, where $f = 9.47 \times 10^{-5}$ s^{-1}). While the traditional theory would have predicted, according to (23) a vertical Ekman-pumping velocity of 1.73 m/day, Ezer and Weatherly found a value of 3.5 m/day, that is, almost exactly double, in perfect agreement with our result.

For a solid-body rotation, we take $\bar{u} = -\Omega y$, $\bar{v} = +\Omega x$, $|\vec{u}| = |\Omega| r$, where Ω is a constant (positive for a cyclone, negative for an anticyclone in the Northern Hemisphere), and r is the radical distance $\sqrt{x^2 + y^2}$. Straightforward calculations yield

$$\bar{w} = \frac{4\kappa^2\lambda|\Omega| r}{\pi^2(1 + \lambda^2)^{3/2} f}(2\Omega + \Omega), \tag{28}$$

where again the first and second terms map those of (25). In this case, we note that the present theory predicts an Ekman-pumping rate 50% greater than that predicted by the traditional theory.

In the case of a zero-vorticity circular flow, we take $\bar{u} = -\Gamma y/r^2$, $\bar{v} = +\Gamma x/r^2$, $|\vec{u}| = |\Gamma|/r$, and find

$$\bar{w} = \frac{4\kappa^2\lambda|\Gamma|}{\pi^2(1 + \lambda^2)^{3/2} fr}\left(0 - \frac{\Gamma}{r^2}\right). \tag{29}$$

Thus, while the traditional theory would have predicted no Ekman pumping (except for an infinite value at the center $r = 0$, where a vorticity singularity exists), the new theory predicts a nonzero Ekman pumping at all distances (and an even stronger singularity at the center). The sign is such that a cyclonic flow in the Northern Hemisphere ($\Gamma > 0$) is accompanied by a downward pumping at finite distances (and an infinite upward pumping at the center). Physically, the absence of vorticity leads to a transverse velocity in the Ekman layer that is not divergent (hence zero pumping according to classic theory), but as the geostrophic velocity decays with radial distance, so does the Ekman-layer thickness. So, unlike the velocity, the volumetric transport is divergent. This divergence is responsible for the Ekman pumping according to the new theory.

A combination of the previous two cases yields a more realistic vortical flow with a nearly solid-body rotation in the center and a zero-vorticity, potential flow at large radial distances:

$$\bar{u} = -\frac{\Gamma y}{R^2 + r^2}, \qquad \bar{v} = +\frac{\Gamma x}{R^2 + r^2},$$
$$|\vec{u}| = \frac{|\Gamma| r}{R^2 + r^2}, \tag{30}$$

where Γ sets the polarity and strength of the vortex, and R the distance over which the transition from solid-body rotation turns into potential flow. Again, r is the radial variable, equal to $\sqrt{x^2 + y^2}$. Calculations yield

$$\bar{w} = \frac{4\kappa^2\lambda|\Gamma| r}{\pi^2(1 + \lambda^2)^{3/2} f(R^2 + r^2)} \times \left[\frac{2\Gamma R^2}{(R^2 + r^2)^2} + \frac{\Gamma(R^2 - r^2)}{(R^2 + r^2)^2}\right], \tag{31}$$

where again the first and second terms correspond to those of (25). Figure 3 compares the prediction of the present theory (sum of both terms) with that of the traditional theory (first term only). Note the significant change in amplitude in the inner part of the vortex and the reversal along its rim.

In the general case of a circular flow with azimuthal velocity $V(r)$ of arbitrary radial profile, the Ekman-pumping velocity is

$$\bar{w} = \frac{4\kappa^2\lambda|V(r)|}{\pi^2(1 + \lambda^2)^{3/2} f}\left[\left(\frac{dV}{dr} + \frac{V}{r}\right) + \frac{dV}{dr}\right], \tag{32}$$

where the term proportional to the relative vorticity $dV/dr + V/r$ would be the sole contribution of the traditional theory. We note that the new theory predicts a larger value (or smaller negative value) where V increases radially, a lower value (or greater negative value) where V decreases radially, and an equal value where V reaches an extremum. For a cyclonic vortex with azimuthal velocity reaching a single maximum at finite distance R from the center, the new theory predicts a stronger upward pumping within the circle of radius R, an equal pumping at R, and a weaker upward pumping or possibly a downward pumping beyond R. Similarly, for an anticyclonic vortex with azimuthal velocity reaching a single maximum at distance R from the center, the new

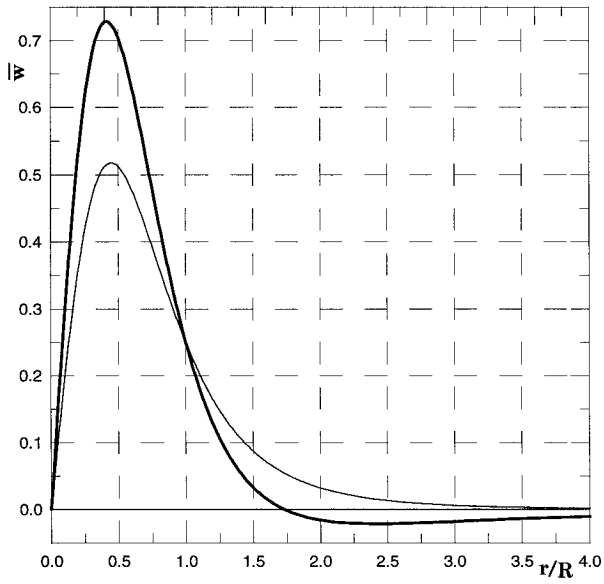

FIG. 3. Radial distributions of the Ekman-pumping vertical velocity for the vortex flow (31), according to the present theory (thick line) and traditional theory (thin line). The present theory predicts an upward velocity that is 41% greater and a weak downward velocity at some distance away from the vortex center. (The vertical axis scale is arbitrary, and only relative variations are significant.)

theory predicts a stronger downward pumping within the circle of radius R, an equal pumping at R, and a weaker downward pumping or possibly an upward pumping beyond R.

4. Conclusions

Our study has revisited the theory of the bottom Ekman layer when the eddy viscosity is made dependent on both the vertical distance from the bottom and the flow magnitude (via the friction velocity); it then recapitulated earlier results and evaluated the resulting Ekman-pumping vertical velocity. A major result is that, because of the dependency of the eddy viscosity on the flow itself, the Ekman-layer thickness increases nearly linearly with the overlying geostrophic current speed, and the volumetric flow carried by the velocity deficit in the Ekman layer is more than proportional to the geostrophic current. From the divergence/convergence of this transverse flow, we derived a new expression for the Ekman-pumping vertical velocity, which is no longer simply proportional to the relative vorticity of the geostrophic current but is a more complicated function of its components and their horizontal derivatives. The full expression is given in (22) with u_* and λ to be derived from (10) and (15). In practice, however, an approximation can be made, and our new formulation can be implemented as follows: Select a bottom roughness height z_0 (usually taken as 5%–10% of the actual height of roughness elements), a value for the Coriolis parameter, and a representative value (scale) of the friction velocity; use (10) to obtain a reference value of λ; then use (24) to obtain the Ekman-pumping rate.

In applying the approximate version of our new expression (i.e., by neglecting the weak variation of λ with the friction velocity), we noted that the Ekman-pumping rate in a unidirectional shear flow is twice that predicted by the traditional theory and is 50% greater in the case of solid-body rotation. For a potential flow (zero relative vorticity), our new expression yields a finite Ekman-pumping rate instead of zero.

We explored how a variation in the formulation of the frictional force impacts the magnitude of the Ekman-pumping vertical velocity. This is by no means the sole modification that can be brought to the traditional bottom Ekman-layer theory. Recently, Hart (1995) considered how the ageostrophic terms in the horizontal-momentum equations modify the Ekman-pumping rate, and he, too, obtained a new expression. It remains now to combine the two modifications in a unified theory, which would rely on neither the assumption of geostrophy or the assumption of constant eddy viscosity, and would be far superior to the traditional theory. Other theoretical generalizations should consider sloping bottoms.

In a final remark, we ask to what extent the ideas and results presented here apply in the presence of vertical stratification and in the presence of convection. In particular, one could explore their application to the atmospheric boundary layer. Such a task falls beyond the scope of the present article and is matter for future work.

Acknowledgments. This research was initiated when the authors participated in a three-week course on environmental physics organized by the International Centre for Theoretical Physics in Trieste, Italy. The authors wish to express their gratitude to the Centre for its hospitality and to the following participants for their helpful suggestions: A. Alonso-Maleta, N. Baybag, and L. Hapolu-Balas. The work was finished at Dartmouth College under Grant N00014-93-1-0391 of the U.S. Office of Naval Research.

APPENDIX

Kelvin-Thomson Functions

The purpose of this appendix is to derive from the Kelvin–Thomson functions of zeroth order two particular functions that form the natural building blocks for the solution of the problem at hand. Some useful properties of these functions are also briefly established.

The Kelvin functions of order zero are the real and imaginary parts of the solutions $w(\eta)$ to the following complex differential equation:

$$\frac{d}{d\eta}\left(\eta\frac{dw}{d\eta}\right) = i\eta w, \tag{A1}$$

where η is real and nonnegative, and i is the imaginary unit (Abramowitz and Stegun 1972, §9.9) [Kelvin functions are occasionally called Thomson functions (Nosova and Basu 1961); recall that William Thomson was Lord Kelvin's earlier name.] Since (A1) is a second-order equation, it admits two independent complex solutions; one solution grows exponentially and the other vanishes for large values of η. The exponentially growing solution finds no place in our boundary-layer analysis and is discarded. Separating the decaying solution into its real and imaginary parts, we write in traditional notation:

$$w(\eta) = \ker_0(\eta) + i\,\mathrm{kei}_0(\eta), \tag{A2}$$

and note the following differential relations obtained from (A1):

$$\frac{d}{d\eta}\left(\eta\frac{d\ker_0}{d\eta}\right) = -\eta\mathrm{kei}_0(\eta) \tag{A3a}$$

$$\frac{d}{d\eta}\left(\eta\frac{d\mathrm{kei}_0}{d\eta}\right) = +\eta\ker_0(\eta). \tag{A3b}$$

Functions better suited to our present problem are obtained with the change of variable $\zeta = \eta^2/4$;

$$a(\zeta) = \ker_0(2\sqrt{\zeta}), \qquad b(\zeta) = \mathrm{kei}_0(2\sqrt{\zeta}), \tag{A4}$$

which obey the differential equations

$$\frac{d}{d\zeta}\left(\zeta\frac{da}{d\zeta}\right) = -b \tag{A5a}$$

$$\frac{d}{d\zeta}\left(\zeta\frac{db}{d\zeta}\right) = +a, \tag{A5b}$$

and vanish for large values of ζ. From the properties of the Kelvin functions $\ker_0(x)$ and $\mathrm{kei}_0(x)$ (Abramowitz and Stegun 1972, §9.9.10 and §9.9.12; Nosova 1961, p. 6), we derive the following expansions near the origin:

$$a(\zeta) = -\frac{1}{2}\ln\zeta - \gamma + \frac{\pi}{4}\zeta + 0(\zeta^2, \zeta^2\ln\zeta) \tag{A6a}$$

$$b(\zeta) = -\frac{1}{2}\zeta\ln\zeta - \frac{\pi}{4} + (1-\gamma)\zeta + 0(\zeta^2, \zeta^3\ln\zeta), \tag{A6b}$$

where γ is the Euler constant ($\gamma = 0.57722$). Thus, the function a has a logarithmic singularity at the origin, while its companion function b does not. The preceding expressions yield the following values at the origin:

$$b(\zeta = 0) = -\frac{\pi}{4}, \qquad \lim_{\zeta\to 0}\zeta\frac{da}{d\zeta} = -\frac{1}{2},$$

$$\lim_{\zeta\to 0}\zeta\frac{db}{d\zeta} = 0. \tag{A7a,b,c}$$

Integration of the differential equations (A5a, b) from zero to infinity with the use of the limits (A7b, c) and of the property that a and b vanish at infinity provides integral values:

$$\int_0^\infty a(\zeta)\,d\zeta = 0, \qquad \int_0^\infty b(\zeta)\,d\zeta = -\frac{1}{2}. \tag{A8a,b}$$

Finally, we note that the functions a and b are linearly independent. Indeed, if they were not, we could write $Aa + Bb = C$, where A, B, and C are nonzero constants. Application of the differential operator $d(\zeta d/d\zeta)/d\zeta$ once and twice yields $-Ab + Ba = 0$ and $Aa + Bb = 0$, respectively. Since a and b are not zero everywhere, it follows that this 2×2 system for A and B must have a zero determinant. Since this determinant is $A^2 + B^2$, it follows that $A = B = 0$, from which also follows $C = 0$. Thus, there is no linear relationship between the two functions.

REFERENCES

Abramowitz, M., and I. A. Stegun, 1972: *Handbook of Mathematical Functions.* 10th ed. Dover, 1046 pp.

Csanady, G. T., and P. T. Shaw, 1980: The evolution of a turbulent Ekman layer. *J. Geophys. Res.*, **85,** 1537–1547.

Cushman-Roisin, B., 1994: *Introduction to Geophysical Fluid Dynamics.* Prentice Hall, 320 pp.

Ellison, T. H., 1956: Atmospheric turbulence. *Surveys in Mechanics, G. I. Taylor Anniversary Volume,* G. K. Batchelor and R. M. Davies, Eds., Cambridge University Press, 400–430.

Ezer, T., and G. L. Weatherly, 1990: A numerical study of the interaction between a deep cold jet and the bottom boundary layer of the ocean. *J. Phys. Oceanogr.*, **20,** 801–816.

Garratt, J. R., 1992: *The Atmospheric Boundary Layer.* Cambridge University Press, 316 pp.

Hart, J. E., 1995: Nonlinear Ekman suction and ageostrophic effects in rapidly rotating fluids. *Geophys. Astrophys. Fluid Dyn.*, **79,** 201–222.

Lavelle, J. W., and H. O. Mofjeld, 1983: Effects of time-varying viscosity on oscillatory turbulent channel flow. *J. Geophys. Res.*, **88,** 7607–7616.

Long, C. E., 1981: A simple model for time-dependent stably stratified turbulent boundary layers. Dept. of Oceanography, University of Washington, Seattle, Special Rep. 95, 23 pp. [Available from University of Washington, WB-10, Seattle, WA 98195.]

Masden, O. S., 1977: A realistic model of the wind-induced Ekman boundary layer. *J. Phys. Oceanogr.*, **7,** 248–255.

Nihoul, J. C. J., 1977: Three-dimensional model of tides and storm surges in a shallow well-mixed continental sea. *Dyn. Atmos. Oceans,* **2,** 29–47.

Nosova, L. N., and P. Basu, 1961: *Tables of Thomson Functions: Their First Derivatives.* Pergamon Press, 422 pp.

Ostendorf, D. W., 1984: The rotary bottom boundary layer. *J. Geophys. Res.*, **89,** 10 461–10 467.

Pedlosky, J., 1987: *Geophysical Fluid Dynamics.* 2d ed. Springer-Verlag, 710 pp.

Soulsby, R. L., 1990: Tidal-current boundary layers. *The Sea,* B. LeMehaute and D. M. Hanes, Eds., Wiley-Interscience, 523–566.

Weatherly, G. L., and P. J. Martin, 1978: On the structure and dynamics of the oceanic bottom boundary layer. *J. Phys. Oceanogr.*, **8,** 557–570.